

Supplement to the manuscript “A scaling approach to project
regional sea-level rise and its uncertainties” submitted to Earth
System Dynamics

Perrette M., Landerer F., Riva R., Frieler, K. and Meinshausen M. (2012)

Table S1: Summary table of the 22 CMIP5 models used in this paper, along with corresponding institutions that provided the model outputs. The “Thermal” and “Dynamic” columns indicate whether the models have been used to compute global mean thermal expansion and dynamic sea-level changes, respectively.

Model name	Thermal	Dynamic	Institution
BCC-CSM1.1	yes	yes	Beijing Climate Center, China Meteorological Administration
BCC-CSM1.1(m)	yes	yes	-
CanESM2	yes	yes	Canadian Centre for Climate Modelling and Analysis
CNRM-CM5	yes	yes	Centre National de Recherches Meteorologiques / Centre Europeen de Recherche et Formation Avancees en Calcul Scientifique
CSIRO-Mk3.6.0	yes	yes	Commonwealth Scientific and Industrial Research Organization in collaboration with Queensland Climate Change Centre of Excellence
FGOALS-s2	no	yes	LASG, Institute of Atmospheric Physics, Chinese Academy of Sciences
GFDL-ESM2G	no	yes	NOAA Geophysical Fluid Dynamics Laboratory
GFDL-ESM2M	no	yes	-
GISS-E2-R	no	yes	NASA Goddard Institute for Space Studies
HadGEM2-CC	yes	no	Met Office Hadley Centre
HadGEM2-ES	yes	yes	-
INM-CM4	yes	no	Institute for Numerical Mathematics
IPSL-CM5A-LR	yes	yes	Institut Pierre-Simon Laplace
IPSL-CM5A-MR	yes	yes	-
MIROC-ESM	yes	yes	Japan Agency for Marine-Earth Science and Technology, Atmosphere and Ocean Research Institute (The University of Tokyo), and National Institute for Environmental Studies
MIROC-ESM-CHEM	yes	yes	-
MIROC5	yes	yes	Atmosphere and Ocean Research Institute (The University of Tokyo), National Institute for Environmental Studies, and Japan Agency for Marine-Earth Science and Technology
MPI-ESM-LR	yes	yes	Max Planck Institute for Meteorology
MPI-ESM-MR	yes	yes	-
MRI-CGCM3	yes	yes	Meteorological Research Institute
NorESM1-M	yes	yes	Norwegian Climate Centre
NorESM1-ME	yes	yes	-

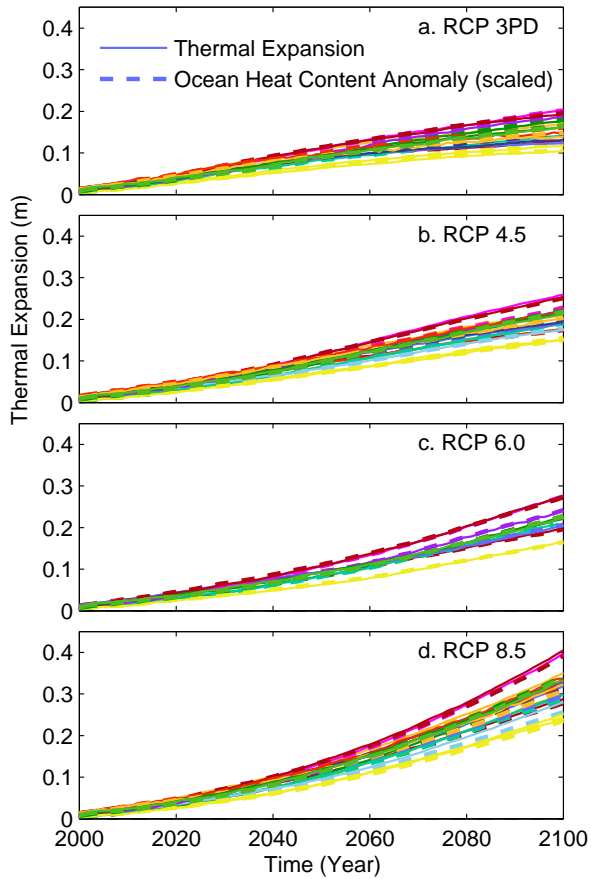


Figure S1: Validation of global mean thermal expansion scaling with the CMIP5 models. For each RCP scenario, direct projection of thermal expansion (thin solid lines) and scaled ocean heat content anomaly (thick dashed lines). The scaling coefficient was obtained from linear regression of the RCP 4.5 scenario, except for MIROC-ESM which is based on RCP6.0 (Fig. 1 in the main manuscript): the very good match of the scaled projections for the other RCP scenarios shows the independence of the scaling coefficient with respect to the emission scenario. The color code is the same as in Figure 1.

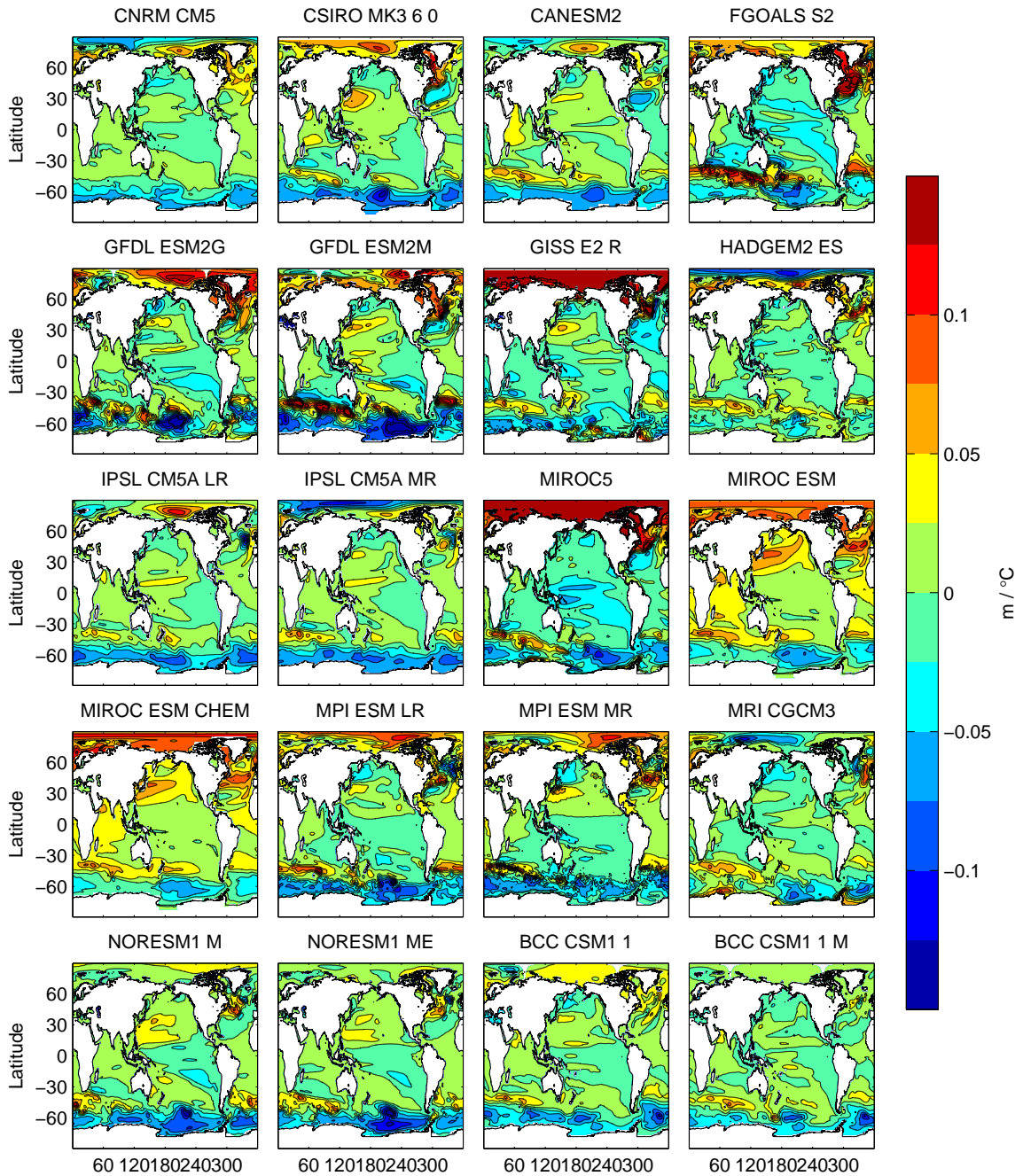


Figure S2: Regression coefficients of dynamic sea-level change against global mean temperature anomaly (in m.K^{-1}) with all combined RCPs over the 2000-2100 period. Contour line intervals are 0.025 m.K^{-1}

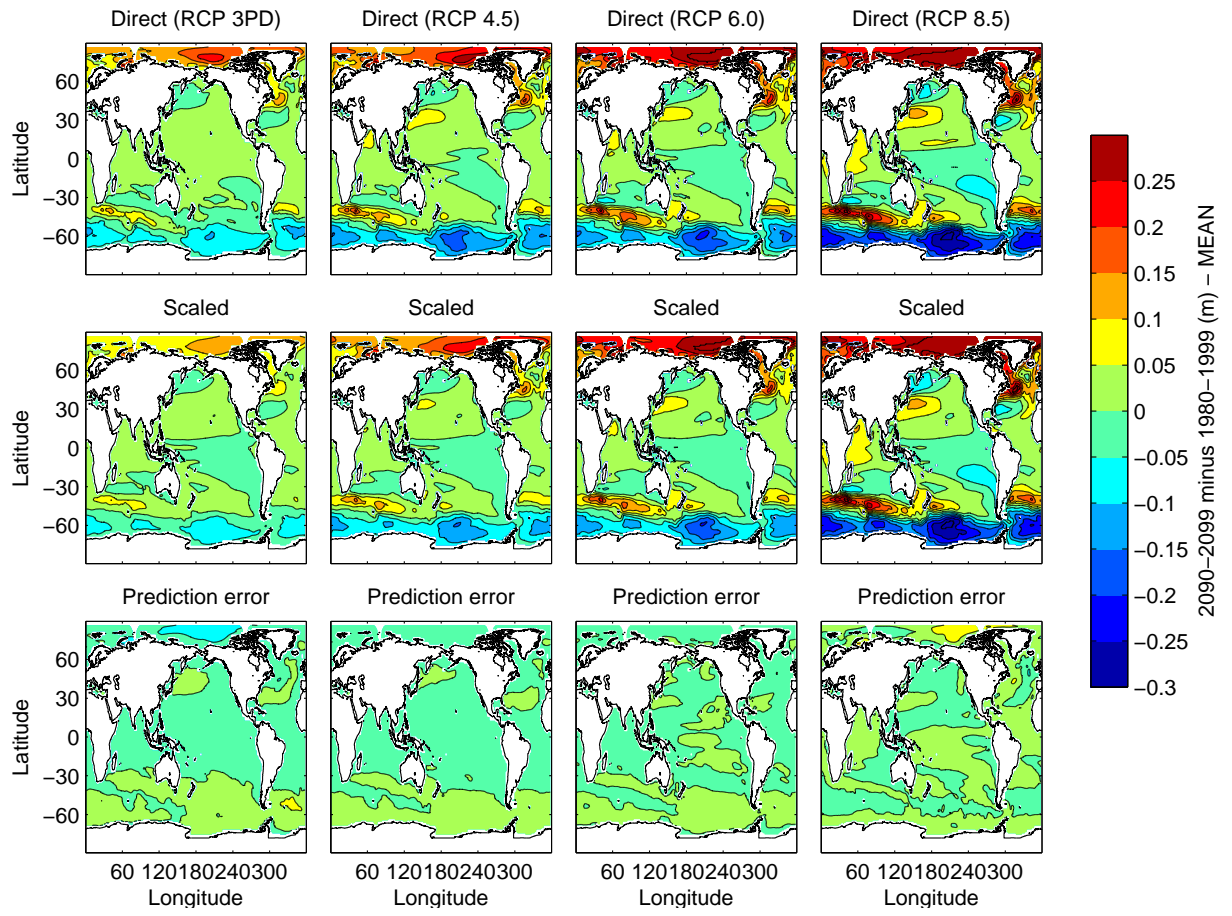


Figure S3: Comparison between multi-model means of direct model projections between 1980-1999 and 2090-2099 averages (top) and multi-model means of scaled projections using the regression method (middle), for the RCP scenarios 3PD, 4.5, 6.0 and 8.5 (from left to right). The difference between the scaled and direct projections is also shown (bottom). Note that for each model, the scaled projections use the same regression pattern for all emission scenarios, derived from all combined RCP scenarios. See also Figure 3 in the main manuscript for a coastline view.

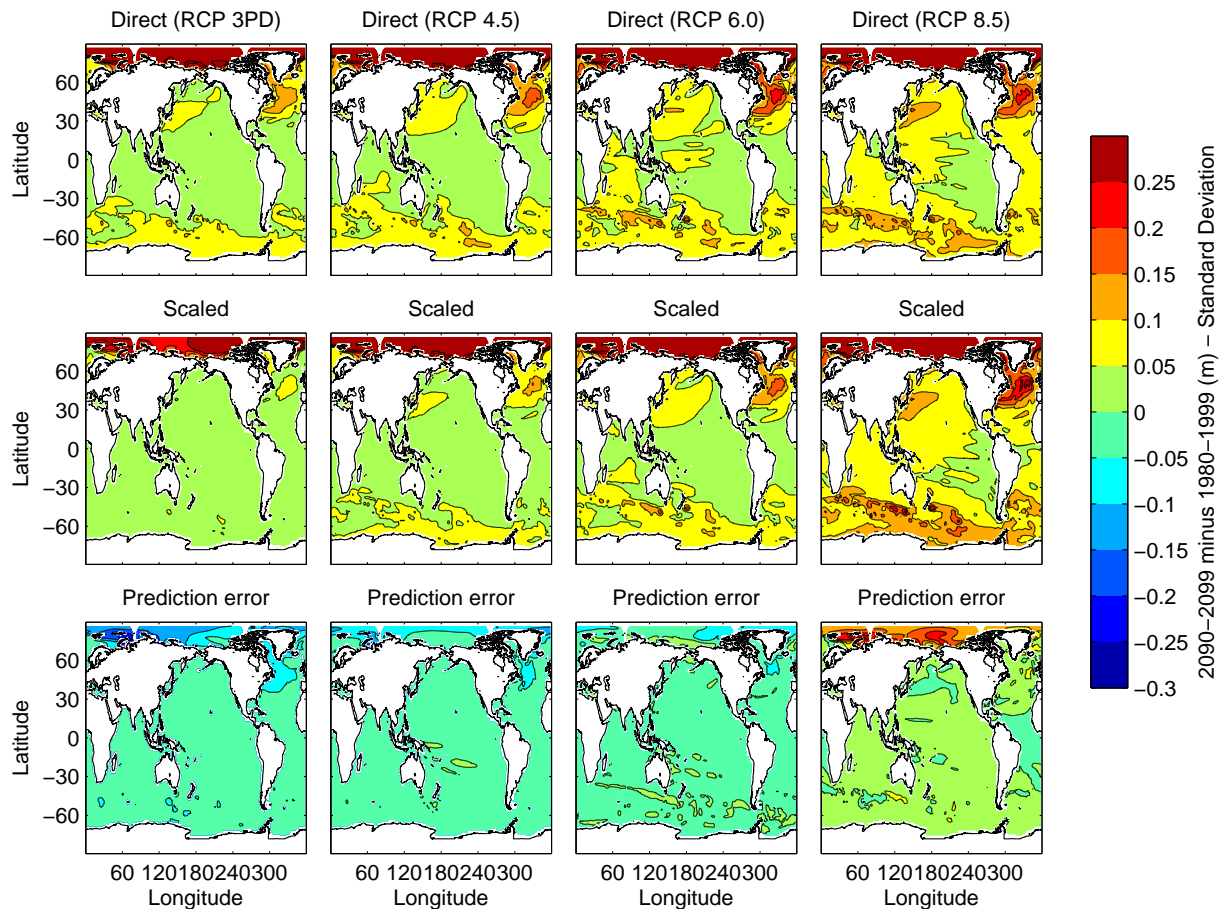


Figure S4: Same as Figure S3 but showing multi-model standard deviations. Positive (negative) values in the last row therefore indicate locations where the multi-model model spread of scaled projections is greater (smaller) than the spread in direct model projection.

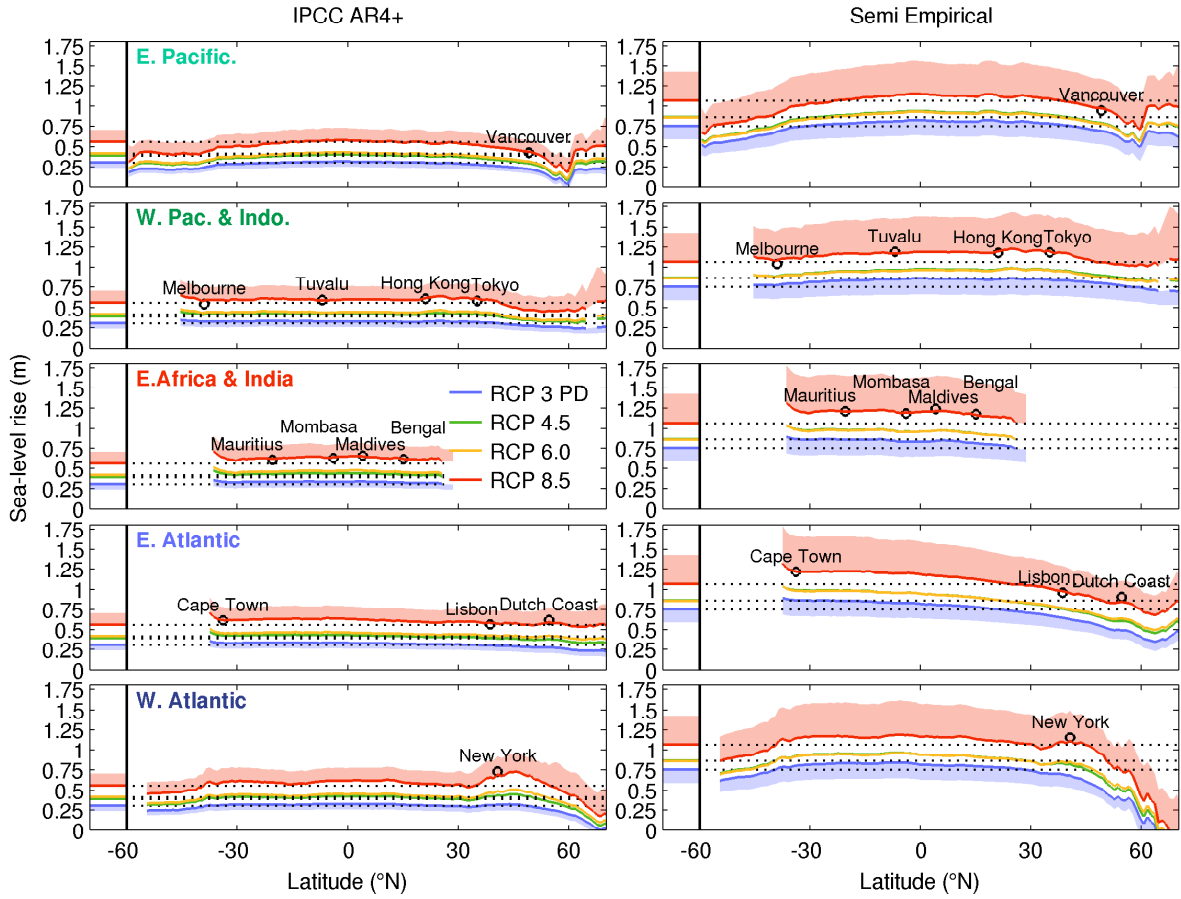


Figure S5: Sea-level rise along the world's coastlines for the four RCP scenarios and the two ice-sheet cases (left: IPCC AR4+, right: Semi-empirical), between 1980-1999 and 2090-2099. The various coastlines are represented in separate panels. Red filled areas represent the upper bound of the uncertainty range in the RCP8.5 scenario (50th to 68th percentiles), and blue filled areas the lower bound in the RCP3PD scenario (16th to 50th percentiles). Global mean sea level rise for each RCP scenario is indicated in the left part of each panel, continued with dotted lines over the rest of the panel. See Figure 9 of the main document to visualize the coastlines on a world map.

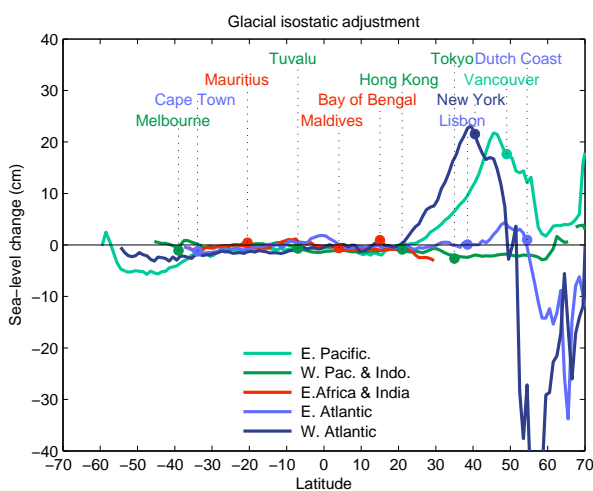
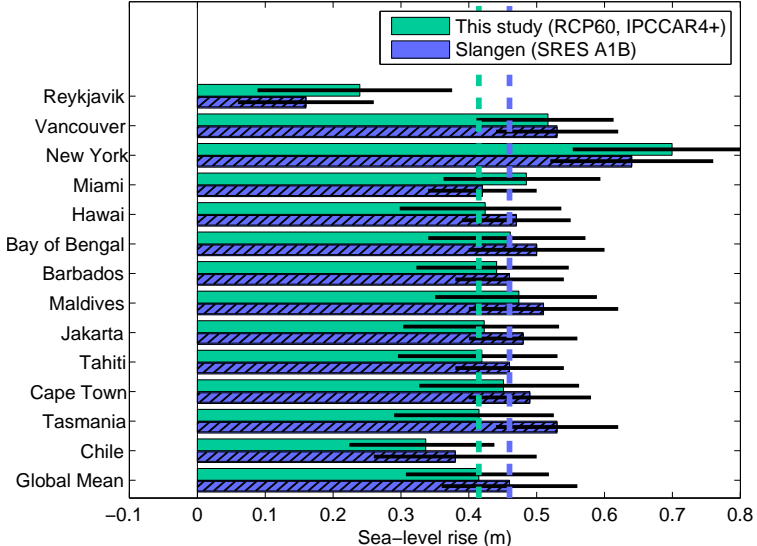
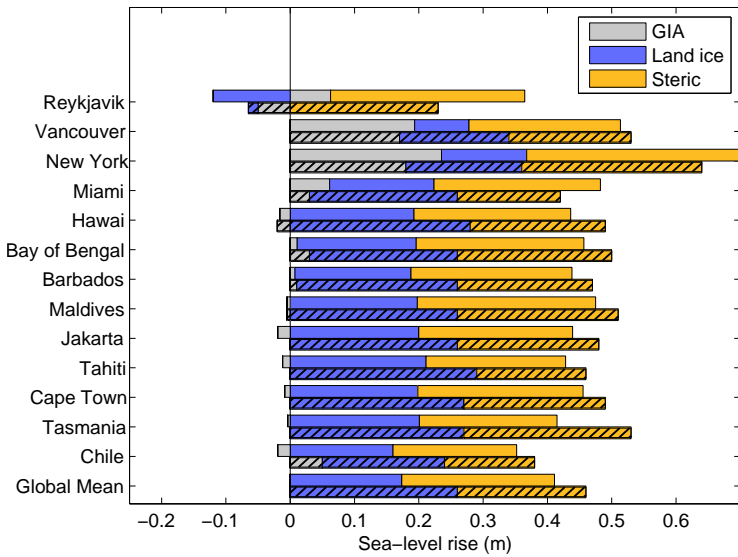


Figure S6: Glacial isostatic adjustment expressed as sea-level change along the world's coastlines, between 1980-1999 and 2090-2099. The data is averaged over a 300 km wide band of coastal waters. Based on ICE-5G (VM2) Peltier (2004).



(a) Total SLR



(b) Individual contributions

Figure S7: Comparison of the IPCCAR+ ice-sheet case (with the RCP 6.0 emission scenario) (filled) with regional SLR projections from Slangen et al. (2011) (with the SRES A1B emission scenario) (hatched). (a) Total SLR with 16th-84th (this study) and 1-sigma uncertainties (Slangen) (both uncertainty measures are equivalent for a Gaussian distribution). (b) Individual contributions to SLR. GIA is included in this figure, to ease comparison (in both cases based on the ICE-5G (VM2) model, but with slightly different implementations). The dashed vertical line in (a) indicated the global mean SLR. The RCP 6.0 emission scenario is comparable to SRES A1B, and the IPCCAR4+ ice sheet case is similar to Slangen et al's treatment of the ice sheets (except that they do consider negative AIS SMB and add a dynamic ice-sheet contribution based on the IPCCAR4 on top of GIS and AIS contribution, which leads to slightly higher ice-sheet contributions than our approach of setting Antarctica contribution to zero and ignoring any dynamic contribution from the ice sheets to SLR). These differences in treatment of the ice sheets, as well as slightly higher MGIC contributions in Slangen et al. (2011) than in our approach, explain the overall higher land-ice contribution in Slangen et al. (2011). Location coordinates may differ between both studies, which is an additional source of discrepancy in regions with small-scale SLR features. We choose this combination of emission scenario and ice-sheet case from our results to help focusing on the regional distribution of SLR. Figures 9 and S5 show a more comprehensive comparison between ice-sheet cases and emission scenarios.

References

- Peltier, W.: Global glacial isostasy and the surface of the ice-age Earth: the ICE-5G (VM2) Model and GRACE, *Annu Rev Earth Planet Sci*, 32, 111–149, doi:10.1146/annurev.earth.32.082503.144359, 2004.
- Slangen, A. B. A., Katsman, C. A., Wal, R. S. W., Vermeersen, L. L. A., and Riva, R. E. M.: Towards regional projections of twenty-first century sea-level change based on IPCC SRES scenarios, *Climate Dynamics*, 38, 1191–1209, doi:10.1007/s00382-011-1057-6, 2011.